Malignant phenotype of renal cell carcinoma cells is switched by Ukrain administration *in vitro*

Nicoletta Gagliano[a], Letizia Pettinari[a], Massimo Aureli[b], Carla Martinelli[a], Elena Colombo[c], Francesco Costa[a], Roberta Carminati[a], Tatiana Volpari[a], Graziano Colombo[d], Aldo Milzani[d], Isabella Dalle-Donne[d] and Magda Gioia[a]

We investigated whether Ukrain modulates the malignant phenotype of clear cell renal cell carcinoma (ccRCC) cells Caki-1, Caki-2, and ACHN treated with four doses (5, 10, 20, and 40 μmol/l) for 24 and 48 h. The epithelial-to-mesenchymal transition markers E-cadherin, β-catenin, and vimentin were analyzed by immunofluorescence as well as actin and tubulin; matrix metalloproteinase-2 and matrix metalloproteinase-9 activity was analyzed by SDS-zymography, intracellular and secreted SPARC levels by western blot, and cell cycle by flow cytometry. Ukrain did not induce E-cadherin/β-catenin immunoreactivity at the cell–cell boundary, although it determined the actin cortical expression in Caki-2 and ACHN, and did not affect vimentin organization; however, in some Caki-1 and ACHN cells the perinuclear concentration of vimentin was consistent with its downregulation. Matrix metalloproteinase-2 and matrix metalloproteinase-9 activity was significantly downregulated 48 h after 20 μmol/l Ukrain administration. At this time point, Ukrain significantly decreased migration and invasion, and downregulated SPARC levels in cell supernatants at all doses in Caki-2, and at 20 μmol/l in Caki-1 and ACHN cells. Concomitantly, SPARC was upregulated in all ccRCC cells, suggesting that Ukrain could also affect cell proliferation by cell cycle inhibition, as supported by the cell cycle analysis, as SPARC also acts as a cell cycle inhibitor. Our results suggest that Ukrain may switch the epithelial-to-mesenchymal transition-related phenotype of ccRCC cells, and targets the two major aspects involved in RCC progression, such as tumor invasion/microenvironment remodeling and cell proliferation. *Anti-Cancer Drugs* 22:749–762 © 2011 Wolters Kluwer Health | Lippincott Williams & Wilkins.

Anti-Cancer Drugs 2011, **22**:749–762

Keywords: cytoskeleton, epithelial-to-mesenchymal transition, matrix metalloproteinases, renal cell carcinoma, secreted protein acidic and rich in cysteine, tumor invasion

Departments of [a]Human Morphology and Biomedical Sciences 'Città Studi', Extracellular Matrix Laboratory, [b]Medical Chemistry, Biochemistry and Biotechnology, [c]Science and Biomedical Technologies, Laboratory of Immunology, School of Medicine, Universita' degli Studi di Milano and [d]Department of Biology, Università degli Studi di Milano, Milan, Italy

Correspondence to Professor Nicoletta Gagliano, PhD, Department of Human Morphology and Biomedical Sciences 'Città Studi', School of Medicine, Università degli Studi di Milano, Via Fratelli Cervi 93, 20090 Segrate – Milan, Italy
Tel: +39 02 50330450; fax: +39 02 50330452;
e-mail: nicoletta.gagliano@unimi.it

Received 1 December 2010 **Revised form accepted** 15 March 2011

Introduction

Renal cell carcinoma (RCC) accounts for 80–85% of kidney tumors, among which 75% are the clear cell type (ccRCC), an aggressive and highly invasive RCC arising from the proximal convoluted tubules, characterized by a 20–30% recurrence after surgical resection and metastatic disease [1,2].

For most carcinomas, malignancy progression is accompanied by the phenotypic switch of differentiated renal tubular epithelial cells to mesenchymal cells, the so-called epithelial-to-mesenchymal transition (EMT) [3,4]. In EMT, the loss of E-cadherin induces the disorganization of the adherens junctions and reduced cell–cell contacts between epithelial cells, largely contributing to the decreased cohesive architecture of normal epithelia. The de-novo expression of vimentin is a molecular marker frequently associated with EMT and the metastatic conversion of epithelial cells. Moreover, a correlation between vimentin expression and a perturbation of E-cadherin-mediated cell adhesion has been evidenced [5]. EMT plays a pivotal role rendering tumor cells invasive and metastatic [3,4]. Phenotypic markers for EMT also comprise an increased capacity for migration and invasion accomplished by extracellular matrix (ECM) breakdown by matrix metalloproteinases (MMPs), leading to cancer cell dissemination and metastases [6].

The anticancer drug Ukrain (NSC 631570) contains alkaloids of greater celandine (*Chelidonium majus*, a member of the Papaveraceae family) [7] and seems to have a potential effect in the treatment of a range of solid tumors including the colon, rectum, breast, pancreas, bladder, and ovary [8–14].

However, the molecular mechanisms of Ukrain-induced antineoplastic effects are not yet completely understood, although an immunostimulating, immunomodulating [15], and antiangiogenic action on human endothelial cells and a proapoptotic action on lymphoma and glioblastoma cells have been reported *in vitro* [16–19].

0959-4973 © 2011 Wolters Kluwer Health | Lippincott Williams & Wilkins DOI: 10.1097/CAD.0b013e328346c7f7

Here, we aimed at investigating whether Ukrain is able to modulate the expression of key markers of EMT and tumor progression *in vitro*, to assess its potential therapeutic effect.

Methods

Cell cultures

Three human ccRCC cell lines were used: Caki-1, Caki-2, and ACHN (American Type Culture Collection, Manassas, Virginia, USA). Cells were cultured in RPMI-1640 supplemented with 10% heat-inactivated fetal bovine serum, 2 mmol/l glutamine, antibiotics (100 U/ml penicillin, 0.1 mg/ml streptomycin), and 0.25 μg/ml amphotericin B.

Ukrain preparation and treatment

Ukrain (kindly provided by Nowicky Pharma, A-1040 Vienna, Austria) was obtained as a 5 mg water-soluble *C. majus* alkaloid thiophosphoric acid derivative in 5 ml of water. ccRCC cells were treated with four final concentrations of Ukrain (5, 10, 20, and 40 μmol/l) for 24 and 48 h in serum-free medium. Untreated cultures served as controls. Each sample was cultured in duplicate.

Cell viability

Cell viability was determined by Trypan blue staining. Cells were plated in 6-well plates (300 000 cells/well) and allowed to attach. Fresh medium containing 5, 10, 20, and 40 μmol/l Ukrain was added, and cells were counted after 0, 24, 48, and 72 h.

Immunofluorescence

Cells were cultured on 12-mm-diameter round glass coverslips in 24-well culture plates. After 24 and 48 h, controls and Ukrain-treated cells were washed in phosphate buffered saline (PBS), fixed in 4% paraformaldehyde in PBS containing 2% sucrose for 5 min at room temperature (RT), postfixed in 70% ethanol, and stored at −20°C until use. The cells were then washed in PBS three times and incubated for 1 h at RT with one of the following monoclonal antibodies: anti-E-cadherin (1 : 500, Becton Dickinson, Buccinasco-Milan, Italy), antivimentin (1 : 100, Novocastra Laboratories, Newcastle upon Tyne, UK), and anti-α-tubulin (1 : 2000, Sigma-Aldrich, Milan, Italy). Secondary antibody conjugated with Alexa 488 (1 : 500, Molecular Probes, Invitrogen, Paisley, UK) was applied for 1 h at RT in the dark. For β-catenin and β-actin analysis, cells were incubated for 1 h with the monoclonal antibody anti-β-catenin (1 : 100, Novocastra Laboratories) or anti-β-actin (1 : 1000, Sigma-Aldrich), respectively. Immunoreactivity was shown with the secondary antibody conjugated with tetramethyl rhodamine iso-thiocyanate (1 : 1000, Molecular Probes, Invitrogen) for 1 h at RT in the dark. In negative controls, the primary antibody was omitted. After the labeling procedure was completed, cells were incubated with 4',6-diamidino-2-phenylindole to stain nuclei (1 : 100 000, Sigma-Aldrich) for 15 min in the dark, and after washing in PBS the coverslips were mounted onto glass slides. The cells were photographed using a digital camera connected to the microscope (Nikon Eclipse E600, Nikon, Melville, New York, USA). Images were processed using specific software (Adobe Photoshop).

SDS-zymography

Culture media were mixed 3 : 1 with sample buffer (containing 10% SDS). Samples (15 μg of total proteins) were run under nonreducing conditions without heat denaturation on 10% polyacrylamide gel (SDS-polyacrylamide gel electrophoresis) copolymerized with 1 mg/ml of type I gelatin. The gels were run at 4°C. After SDS-polyacrylamide gel electrophoresis, the gels were washed twice in 2.5% Triton X-100 for 30 min each and incubated overnight in a substrate buffer at 37°C (Tris–HCl 50 mmol/l, $CaCl_2$ 5 mmol/l, NaN_3 0.02%, pH 7.5). MMP gelatinolytic activity, detected after staining the gels with Coomassie Brilliant Blue R250 as clear bands on a blue background, was quantified by densitometric scanning (UVBand, Eppendorf, Milan, Italy).

Migration and invasion assay

Migration assay was performed using transwell inserts (6.5 mm insert diameter, 8 μm pore size) (Corning, New York, USA), placed in 24-well cell culture plates. In brief, 100 μl of a suspension with 1×10^5 cell/ml in serum-free RPMI-1640 containing controls or Ukrain-treated cells was added to the top cell culture insert. RPMI-1640 containing 10% serum in the presence or absence of Ukrain at the same concentration of the insert was applied to the wells in which the top cell culture inserts containing cells were placed. Cell migration through the membrane was assessed by staining the cells that attached to the lower and the upper sides of the membrane with calcein-AM (3 μg/ml in PBS) for 30 min at 37°C, 5% CO_2. After staining, cells derived from the upper and the lower sides of the membrane were detached using trypsin, separately transferred into a clean tube, then centrifuged, lysed, and transferred to the black module strip. Fluorescence was measured at 485 nm (excitation) and 520 nm (emission). As a background, calcein-AM was incubated without cells. The number of migrating and nonmigrating cells was expressed as relative fluorescence units and the results were calculated as migration rate in relation to the total number of cells.

The invasive potential of controls and Ukrain-treated cells was assessed using the same transwell inserts coated with basement membrane matrix (Geltrex, Gibco, Paisley, UK) according to the manufacturer's instructions. The experimental procedures were the same as for the migration assay, and the number of cells able to invade through the matrigel and noninvading cells was calculated as invasion rate in relation to the total number of cells.

Each experimental point was run in duplicate, and data were expressed as the mean values ± standard deviation of three independent experiments.

Western blot

Cell lysates (40–60 μg) or culture media (15 μg of total proteins) were separated by 10% SDS-PAGE, and transferred at 90 V to a nitrocellulose membrane in 0.025 mol/l Tris, 192 mmol/l glycine, 20% methanol, pH 8.3. After electroblotting, the membranes were air dried and blocked for 1 h with 5% skim milk in Tris-buffered saline and Tween 20 and incubated for 1 h in monoclonal antibody to vimentin (1 : 1000, Novocastra Laboratories). To confirm equal loading, membranes were reprobed by monoclonal antibody to α-tubulin (1 : 2000 dilution, Sigma-Aldrich).

For secreted protein acidic and rich in cysteine (SPARC) analysis, membranes were incubated for 1 h at RT in monoclonal antibody to SPARC (1 : 100 in Tris-buffered saline and Tween 20, Novocastra Laboratories), and after washing, in horseradish peroxidase-conjugated rabbit antimouse serum (1 : 6000 dilution, Sigma-Aldrich). Immunoreactive bands, shown using the Opti-4CN substrate (Bio Rad, Segrate-Milan, Italy), were scanned densitometrically (UVBand, Eppendorf).

Cell cycle analysis

The cell phase distribution 48 h after Ukrain treatment was assayed by determination of the DNA content as previously described [20]. Cells were trypsinized (trypsin 0.025%; EDTA 0.01% in PBS), fixed in 70% ethanol at −20°C, treated with 100 μg/ml RNase A for 30 min at 37°C, stained with 1 ml of a solution containing propidium iodide (50 μg/ml) in PBS and RNase A (100 μg/ml), and maintained at 4°C for at least 12 h. Monoparametric cell cycle analysis was performed on at least 2×10^4 cells for each sample using an FacsCanto II instrument equipped with FacsDiva 6.1 Software (Becton Dickinson) and the distribution of the different cell cycle phases was calculated.

Annexin V

The apoptosis ratio in controls and Ukrain-treated cells was analyzed at the time points of 24 and 48 h using the Annexin V-FITC Apoptosis Detection Kit (Calbiochem, Nottingham, UK) according to the manufacturer's instructions.

Statistical analysis

Data, expressed by mean ± standard deviation, were analyzed by one-way analysis of variance and the Student–Neumann–Keuls post hoc test (Prism GraphPad). *P* values of less than 0.05 were considered significant.

Results

Cell viability and proliferation

Ukrain administration dose-dependently decreased cell proliferation in all three cell lines (Fig. 1). Inhibition of cell proliferation was evident 24 h after 10, 20, and 40 μmol/l Ukrain administration, and 48 h after all doses of Ukrain. The administration of 40 μmol/l Ukrain induced the death of all ACHN cells 48 h after treatment. Therefore, we investigated whether the drug was effective in inducing apoptosis by analyzing annexin V expression. Our results point to a dose-dependent increase of the number of apoptotic cells after both the 24 and the 48 h time points (Fig. 2).

Fig. 1

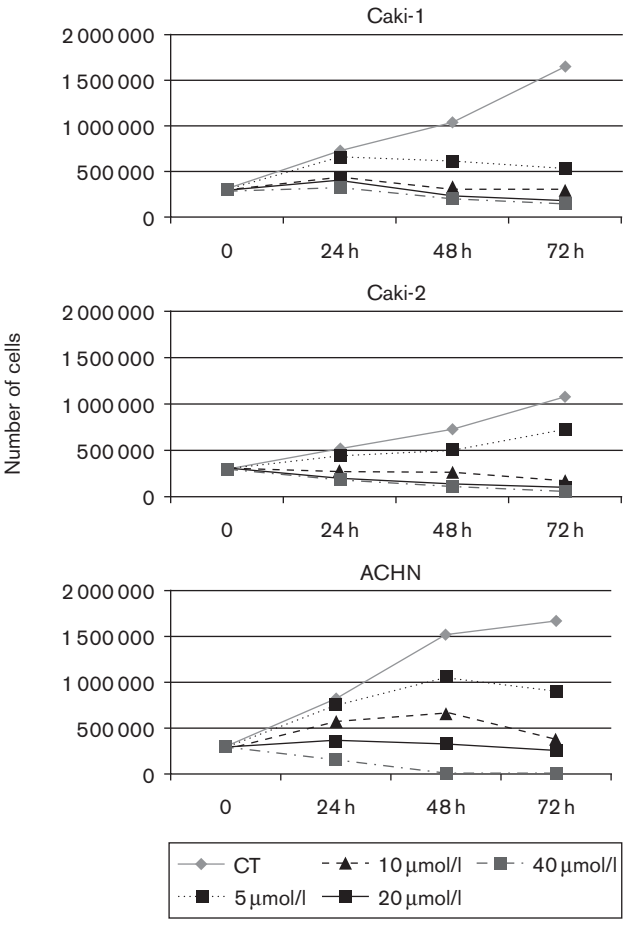

Time-dependent effect of Ukrain on cultured ccRCC cell proliferation. Cells were plated in 6-well plates (300 000 cells/well) and allowed to attach. Fresh medium containing 5, 10, 20, and 40 μmol/l Ukrain was added, and cells were counted at the times indicated. Untreated ccRCC cells were used as controls (CT). Inhibition of cell proliferation was evident 24 h after 10, 20 and 40 μmol/l Ukrain administration, and 48 h after all doses of Ukrain. After 10 and 20 μmol/l Ukrain administration, cell proliferation was completely inhibited in all ccRCC cell lines. Each time point represents the mean of triplicate samples.

Fig. 2

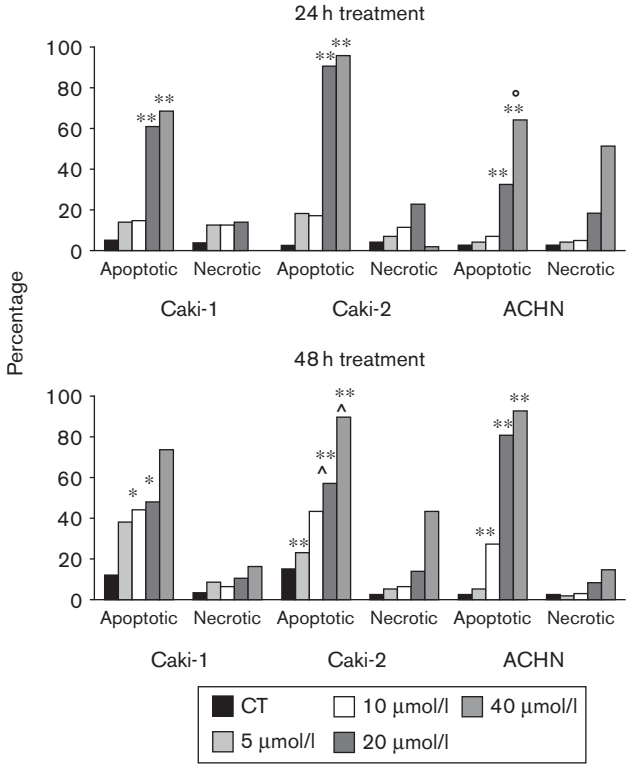

Percentages of apoptotic and necrotic cells after Ukrain administration measured using the annexin V-FITC-PI kit after 24 and 48 h. Annexin V-FITC and propidium iodide (PI) double stain were used to evaluate the percentages of apoptosis. Annexin V+ and PI− cells were designated as apoptotic, and Annexin V+ and PI+ cells showed necrosis. Ukrain significantly increased the percentage of apoptotic cells starting from 10 μmol/l Ukrain in Caki-1, and from 5 μmol/l Ukrain in Caki-2 and ACHN. Tests were repeated in triplicate. *$P<0.05$ vs. control (CT); **$P<0.005$ vs. CT; ^$P<0.05$ vs. Ukrain 5 μmol/l; °$P<0.05$ vs. Ukrain 20 μmol/l.

Cell morphology

Cell morphology was similarly affected by Ukrain administration after 24 (data not shown) and 48 h (Fig. 3). Morphological changes occurred in Caki-1 and ACHN cells after Ukrain administration. Untreated Caki-1 and ACHN grew as loosely adherent spindle-shaped, fibroblast-like cells suggestive of a mesenchymal phenotype. After Ukrain administration, they tended to grow as fairly tight aggregates, in which cells showed a rounded polygonal shape consistent with a more epithelial-like phenotype. By contrast, Caki-2 cells are small polygonal growing cells forming small aggregates whose appearance is not modified after Ukrain administration. Figure 3 shows that 48 h after administration of 40 μmol/l Ukrain, the most part of Caki-1 and Caki-2 cells are dead, while at this time point Ukrain killed all ACHN cells. As a consequence, all the immunofluorescence and molecular evaluations at the 48 h time point were performed on cells after Ukrain 5, 10, and 20 μmol/l administration.

Immunofluorescence analysis for tubulin showed that microtubule cytoskeleton remained preserved in all controls and Ukrain-treated cells (Fig. 4).

Epithelial-to-mesenchymal transition markers

E-cadherin is a transmembrane glycoprotein whose cytoplasmic domain is complexed with β-catenin. When during EMT the loss or cleavage of E-cadherin occurs, β-catenin internalization is promoted. We analyzed E-cadherin and β-catenin expression and localization in ccRCC cells. Their pattern of expression was very similar to both 24 and 48 h after Ukrain administration. In Caki-2 cells (Fig. 5), both E-cadherin and β-catenin immunoreactivity were similarly expressed in the cytoplasm of controls and Ukrain-treated cells. Hence, Ukrain seems to be unable to induce junctional localization of these proteins to the cell–cell contact sites as in normally differentiated epithelial cells. A similar pattern was observed for Caki-1 and ACHN (Fig. 5).

In all controls, a diffuse pattern consisting of actin stress fibers was evident (Fig. 6). Ukrain administration did not affect actin filament arrangement in Caki-1. In contrast, in Caki-2 and ACHN cells, Ukrain induced actin expression at the boundary between cells starting after 5 μmol/l and 10 μmol/l Ukrain, respectively, suggesting that Ukrain administration elicits actin cytoskeleton reorganization in ccRCC cells. This effect was observed in some ACHN cells 24 h after 20 and 40 μmol/l Ukrain administration (data not shown).

The majority of the cells showed vimentin dispersed filaments, typical of the vimentin network (Fig. 7). Both in controls and Ukrain-treated cells, vimentin filaments were found around the nucleus, from which they irradiated out into the cell periphery in fine lace-like threads (see the representative box in Fig. 7), suggesting that Ukrain does not affect the vimentin organization, typical of mesenchymal cells. Western blot analysis confirmed that vimentin expression is not quantitatively affected by Ukrain (Fig. 8). However, few Caki-1 and ACHN cells starting after 5 μmol/l Ukrain administration showed a perinuclear concentration of vimentin immunoreactivity with only limited filamentous extension, consistent with a downregulation of the protein [21] (Fig. 7, arrows). Hence, although in some cells vimentin seems downregulated by Ukrain, western blot analysis shows that Ukrain is not able to decrease the overall vimentin expression in Caki-1 and ACHN cells. In Caki-2 cells, vimentin expression slightly tended to increase 48 h after 10 and 20 μmol/l Ukrain administration, but this pattern is not statistically significant.

Matrix metalloproteinase activity

MMP activity was analyzed by SDS-zymography. Densitomentric analysis of the zymograms showing MMP-2 and MMP-9 activity 24 h after Ukrain treatment shows that at

Fig. 3

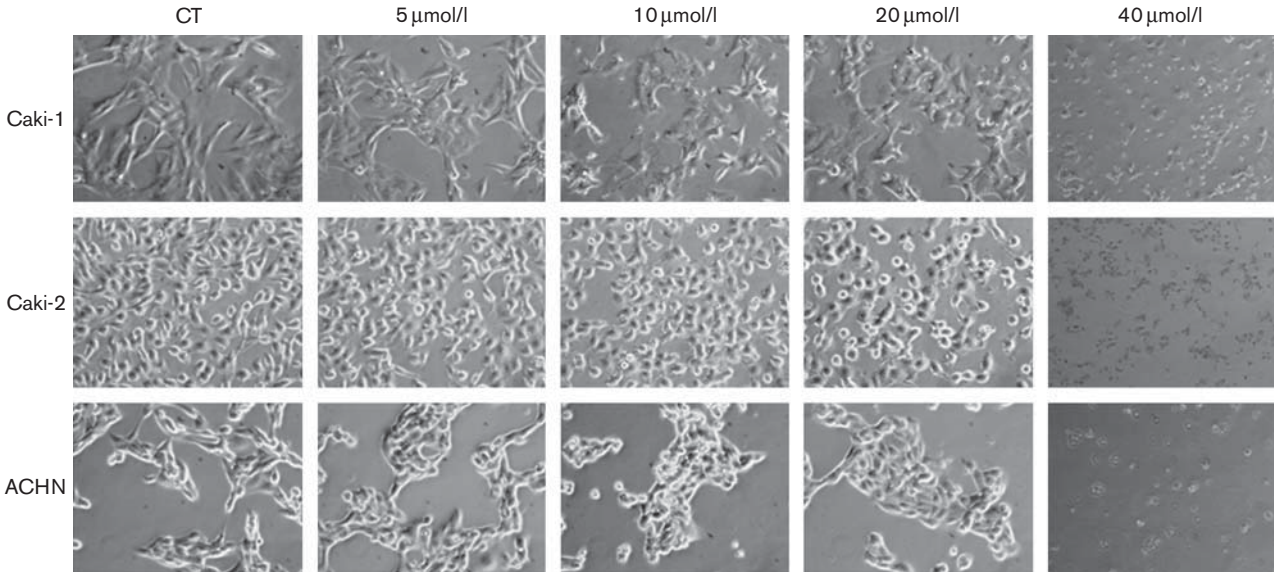

Microphotographs showing cell morphology of control (CT) and Ukrain-treated cells after 48 h. Untreated Caki-1 and ACHN are loosely adherent spindle-shaped, fibroblast-like cells, suggestive of a mesenchymal phenotype, but after Ukrain administration they tended to show a more rounded polygonal shape consistent with an epithelial-like phenotype. In contrast, Caki-2 morphology was not modified after Ukrain administration. Original magnification: × 20 for CT and 5, 10, and 20 μmol/l Ukrain-treated cells. For the 40 μmol/l treatment, the original magnification was ×10 to show that Ukrain administration induces cell death in most cells. At this dose, Ukrain killed all ACHN cells that were round and floating in the cell culture medium.

Fig. 4

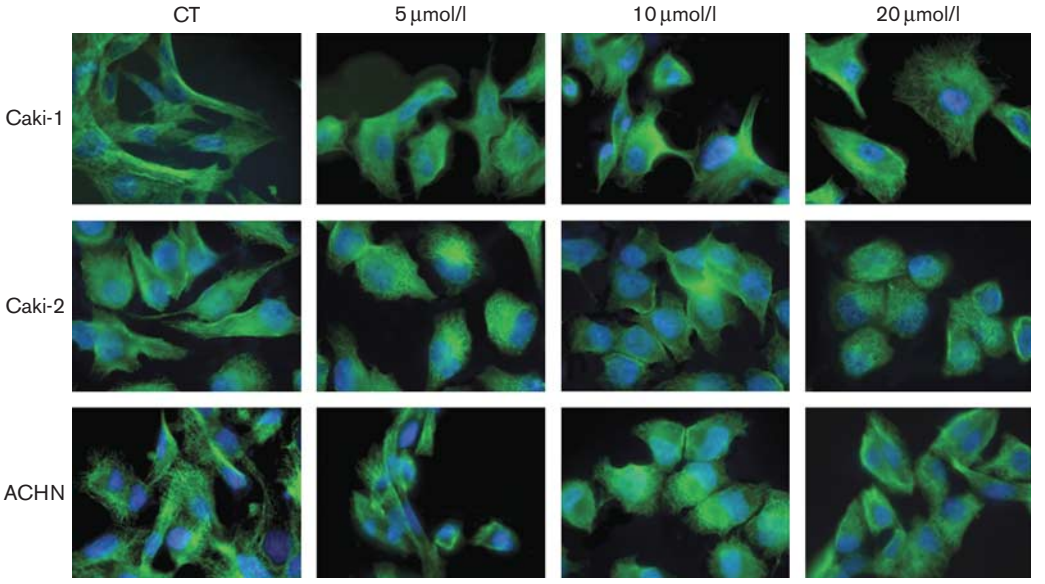

Representative immunofluorescence analysis showing tubulin cytoskeleton organization in Caki-1, Caki-2, and ACHN ccRCC cells. Our data showed that tubulin expression is not modified 48 h after Ukrain treatment, and showed the absence of abnormal mitosis, thus suggesting that the antimitotic and antiproliferative effect of Ukrain is not based on tubulin cytoskeleton alteration. Green: tubulin; blue: 4′,6-diamidino-2-phenylindole. Original magnification: ×100.

this time point supernatants of controls and Ukrain-treated cells have the same gelatinase activity (Fig. 9b). Forty-eight hours after Ukrain administration, MMP-2 activity (Fig. 9a and b) in cell supernatants strongly decreased after Ukrain 20 μmol/l in Caki-1 ($P < 0.0005$ for Ukrain 20 μmol/l vs. 10 μmol/l, $P < 0.005$ for Ukrain

Fig. 5

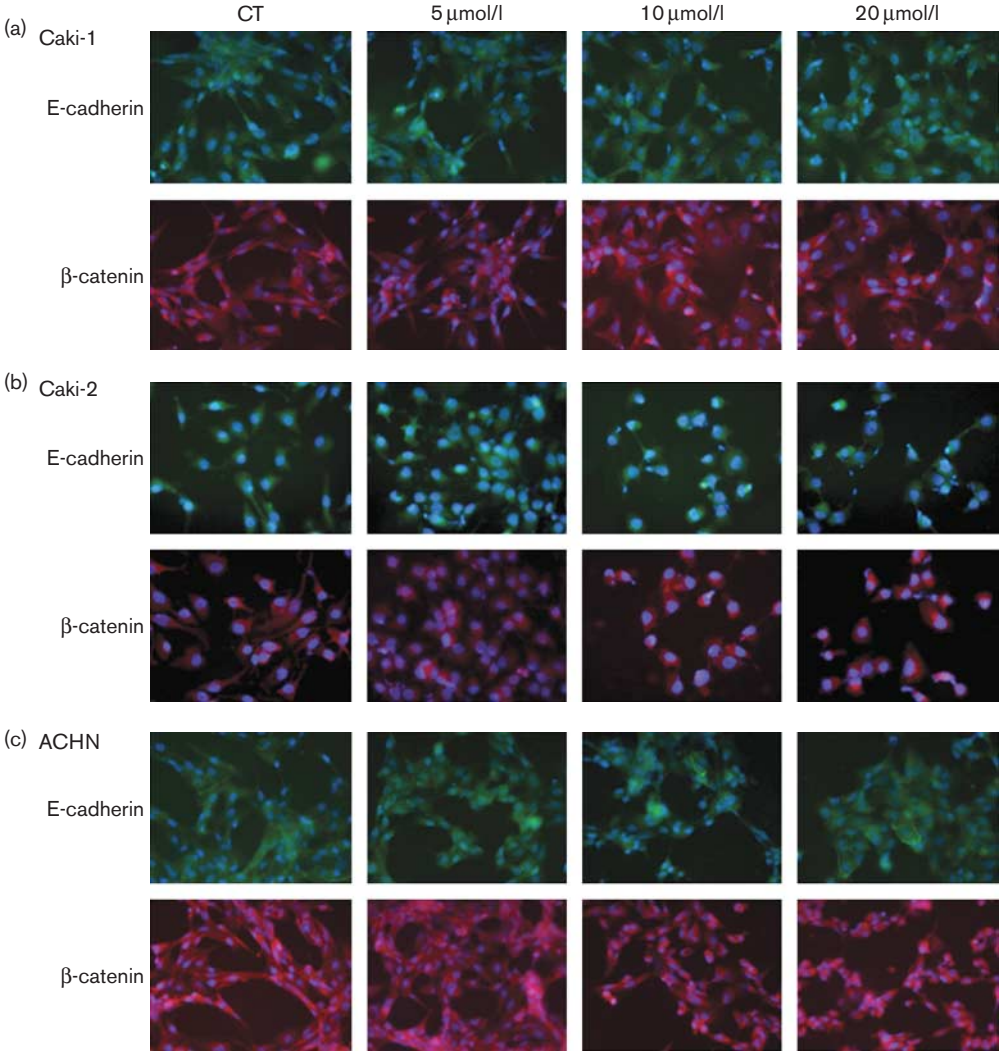

Representative immunofluorescence analysis showing E-cadherin and β-catenin expression and localization in Caki-1 (a), Caki-2 (b), and ACHN (c) ccRCC cells after 48 h. Both E-cadherin and β-catenin immunoreactivity, expressed at a similar extent in control (CT) and Ukrain-treated cells, were observed in the cytoplasm and were not localized at the plasma membrane level after Ukrain treatment. Green: E-cadherin; red: β-catenin; blue: 4′,6-diamidino-2-phenylindole. Original magnification: ×40.

20 μmol/l vs. controls and 5 μmol/l), in Caki-2 ($P < 0.005$ for Ukrain 20 μmol/l vs. controls and 10 μmol/l), and ACHN ($P < 0.005$ for Ukrain 20 μmol/l vs. controls). MMP-9 activity was significantly downregulated by Ukrain in Caki-1 ($P < 0.0005$ for Ukrain 20 μmol/l vs. 10 μmol/l, $P < 0.005$ for Ukrain 20 μmol/l vs. controls 5 μmol/l), and tended to drop after Ukrain 20 μmol/l administration in Caki-2 and ACHN cells (P not significant).

Migration and invasion assay

As differences in MMPs activity between controls and Ukrain-treated samples were not found 24 h after Ukrain administration, the functional migration and invasion assays were performed on samples treated for 48 h. The migration rate (Fig. 10a) was strongly reduced by Ukrain in Caki-1 ($P < 0.05$ for Ukrain 5 and 20 μmol/l vs. controls), Caki-2 ($P < 0.0005$ for Ukrain 20 μmol/l vs. controls, 5 and 10 μmol/l, $P < 0.05$ for controls vs. Ukrain 5 and 10 μmol/l), and ACHN cells ($P < 0.005$ for Ukrain 10 and 20 vs. 5 μmol/l).

Ukrain also induced a significant decrease of the percentage of invading cells (Fig. 10b) (for Caki-1, Caki-2, and ACHN $P < 0.005$ for Ukrain 10 and 20 μmol/l vs. controls; for Caki-1 and Caki-2 $P < 0.05$ for Ukrain 5 μmol/l vs. controls).

Secreted protein acidic and rich in cysteine expression

SPARC expression was analyzed both in cell culture supernatants and at the intracellular level. Twenty-four

Fig. 6

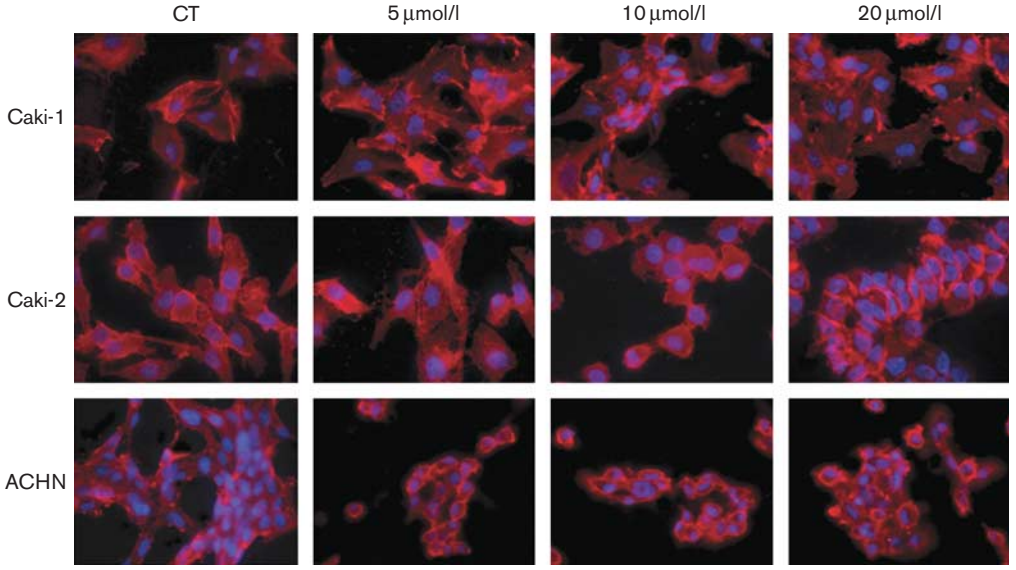

Representative immunofluorescence analysis showing the actin cytoskeleton arrangement in control (CT) and Ukrain-treated ccRCC cells. In CT, a diffuse pattern of actin arrangement consisting of stress fibers was observed. Forty-eight hours after Ukrain administration, actin filaments tended to be localized at the boundary at the cell–cell contacts in Caki-2 and ACHN cells, suggesting that Ukrain administration induced a reorganization of the actin cytoskeleton consistent with a more epithelial-like phenotype. Caki-1 cells were not affected by Ukrain treatment. Red: actin; blue: 4′,6-diamidino-2-phenylindole. Original magnification: ×60.

Fig. 7

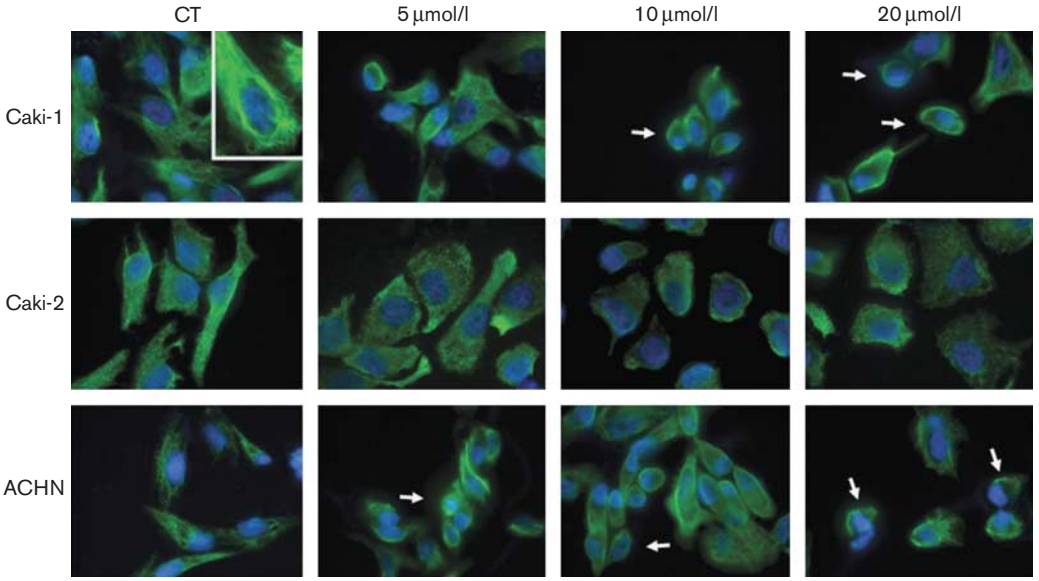

Representative immunofluorescence analysis for vimentin-intermediated filaments in control (CT) and Ukrain-treated ccRCC cells after 48 h. After Ukrain administration, vimentin immunoreactivity was unchanged, although in some Caki-1 and ACHN cells (arrows) the filaments are condensed in the perinuclear region, suggesting vimentin downregulation. Green: vimentin; blue: 4′,6-diamidino-2-phenylindole. Original magnification: ×100.

hours after Ukrain administration, SPARC expression was significantly affected only in ACHN. In fact, the drug induced the upregulation of the SPARC intracellular levels ($P < 0.05$ for 20 and 40 μmol/l Ukrain vs controls, 10 μmol/l and 5 μmol/l) and the concomitant downregulation in cell supernatants ($P < 0.05$ for 20 and 40 μmol/l Ukrain vs controls). After 48 h, SPARC expression in cell lysates that tended to be upregulated in Ukrain-treated

Fig. 8

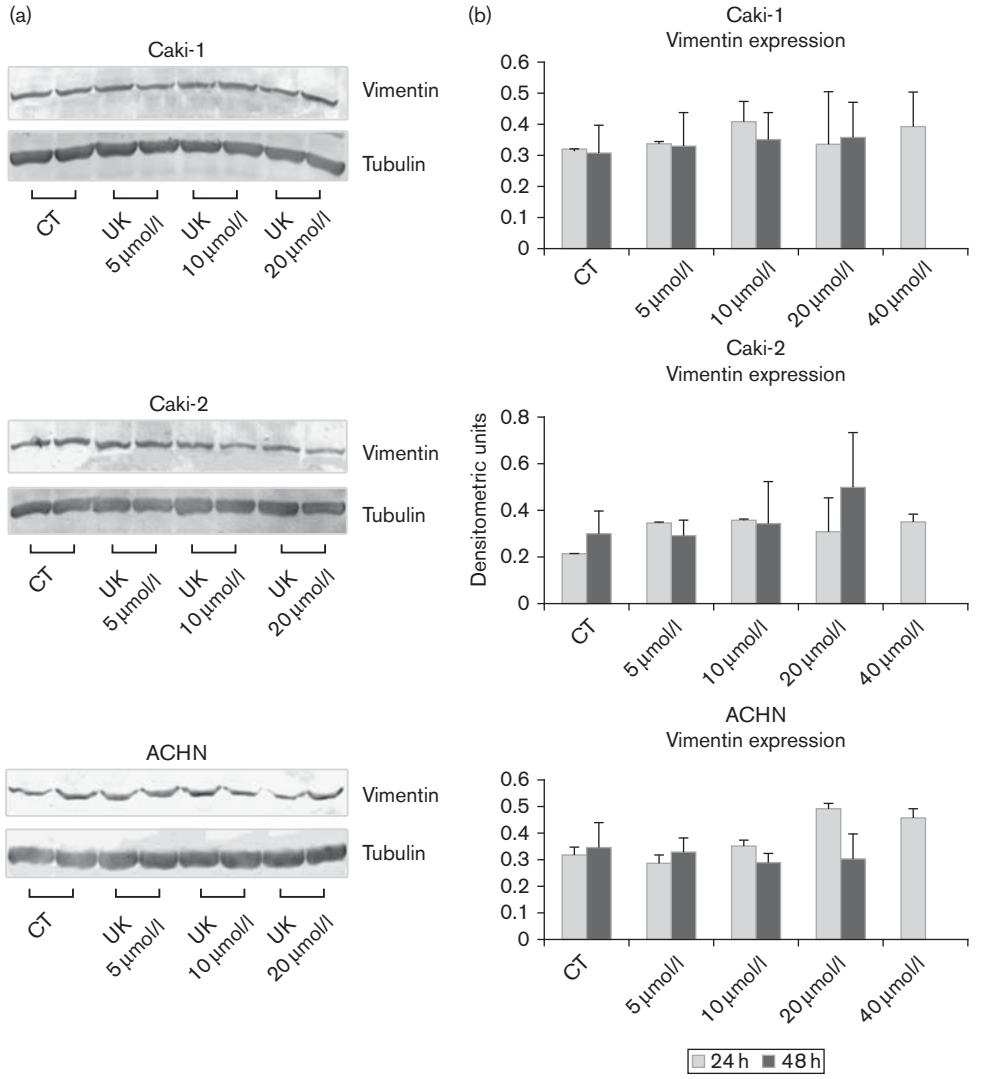

(a) Representative western blot for vimentin in cell lysates 48 h after Ukrain administration. Membranes were normalized using an antitubulin antibody. (b) Bar graphs showing vimentin expression after densitometric scanning of immunoreactive bands at both the considered time points. Forty-eight hours after treatment Ukrain is not able to decrease the overall vimentin expression in all the considered ccRCC cells. Data were obtained from three independent experiments for samples run in duplicate and are expressed as densitometric units ± standard deviation.

Caki-1, was significantly increased after Ukrain 20 μmol/l in Caki-2 compared with controls ($P < 0.05$), and resulted unchanged in ACHN cells, although in this cell line Ukrain induced a significant increase of SPARC 24 h after 20 and 40 μmol/l Ukrain administration (Fig. 11a).

In contrast, SPARC protein levels in cell supernatants showed an opposite pattern of expression 48 h after Ukrain administration. In fact, SPARC protein levels strongly decreased in Caki-1 after 20 μmol/l Ukrain administration ($P < 0.005$ for Ukrain 20 μmol/l vs. controls; $P < 0.05$ for Ukrain 20 vs. 10 and 5 μmol/l), in Caki-2 ($P < 0.0005$ for Ukrain 5 and 10 μmol/l vs. controls, $P < 0.005$ for Ukrain 20 μmol/l vs. controls), and in ACHN ($P < 0.05$ for Ukrain 20 μmol/l vs. controls, $P < 0.005$ for Ukrain 20 μmol/l vs. Ukrain 5 and 10 μmol/l) (Fig. 11b).

Cell cycle analysis

Flow cytometry analysis of the DNA content showed a G2/M phase cell cycle arrest after Ukrain treatment (Table 1). The percentage of cells in G2/M increased 48 h after Ukrain administration, and this effect was evident after Ukrain 20 μmol/l treatment. These results indicate that Ukrain primarily induced G2/M phase arrest in ccRCC cancer cells.

Fig. 9

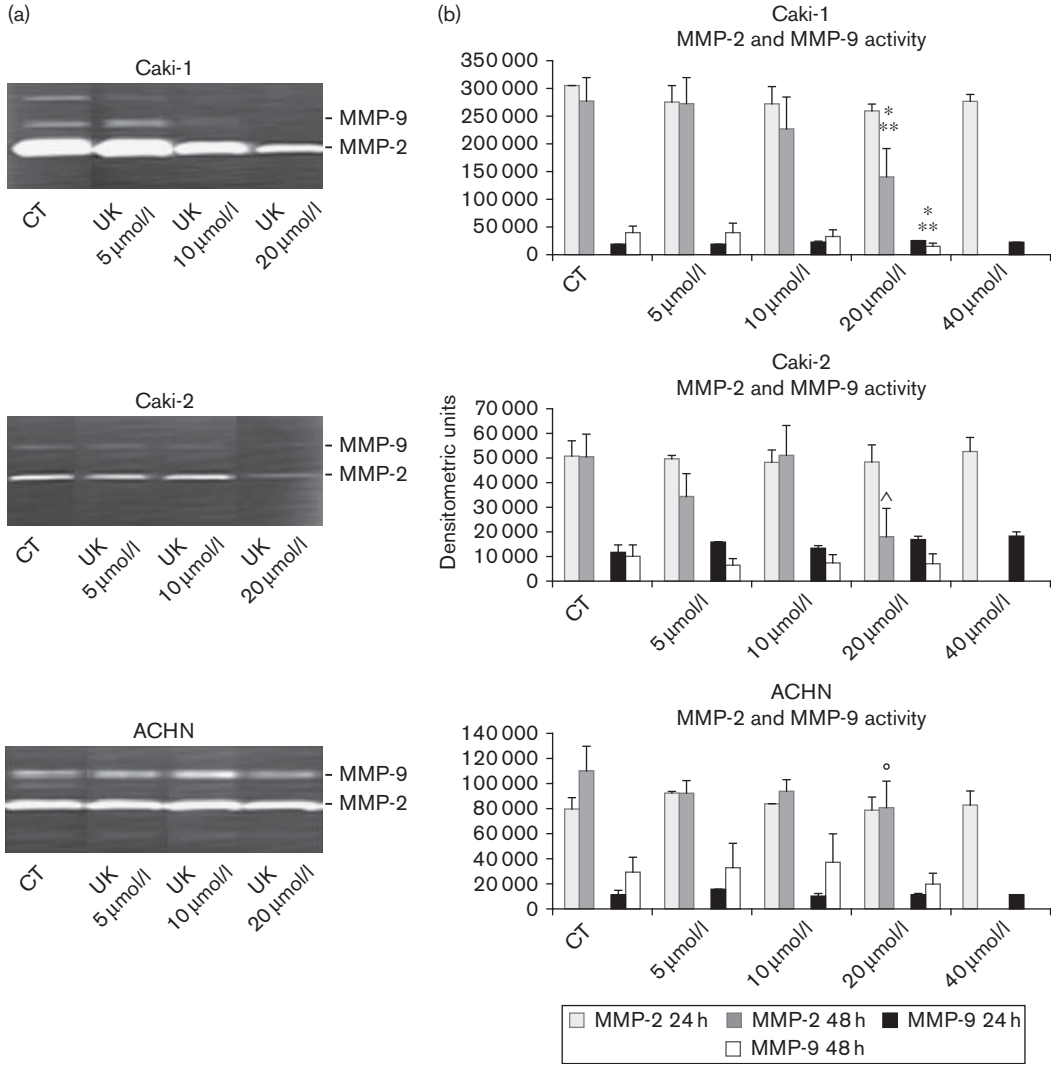

(a) Representative gelatin zymograms of matrix metalloproteinases (MMPs) in serum-free, conditioned human ccRCC cell supernatants from CT and Ukrain-treated cells after 48 h. The lytic bands weighing 72 kDa and in the 90 kDa region are consistent with proMMP-2 and proMMP-9, respectively. (b) Bar graphs showing proMMP-2 and proMMP-9 activity in Caki-1, Caki-2, and ACHN serum-free conditioned media after densitometric analysis of lytic bands following SDS-zymography. Our results show that Ukrain significantly affects MMP-2 and MMP-9 activity, suggesting that this drug may elicit a relevant effect on the mechanisms responsible for tumor invasion. Data are expressed as densitometric units ± standard deviation for three independent experiments for samples run in duplicate. *$P<0.0005$ vs. 10 µmol/l; **$P<0.005$ vs. CT and 5 µmol/l; ^$P<0.005$ vs. CT and 10 µmol/l; and °$P<0.005$ vs. CT.

Discussion

Progression of carcinomas is accompanied by EMT, leading to the loss of epithelial characteristics and the acquisition of a mesenchymal phenotype that play a pivotal role rendering tumor cells invasive and able to disseminate forming metastasis.

We investigated *in vitro* whether Ukrain affects ccRCC cell proliferation and the expression of EMT markers and of genes and proteins involved in the mechanisms leading to tumor invasion. Ukrain dose-dependently reduced ccRCC cell proliferation 24, 48, and 72 h after treatment. This was evident after the 10 µmol/l dose and suggests that the drug has a cytostatic effect possibly elicited, according to previous findings, by inhibition of DNA, RNA, and protein synthesis, and by the induction of apoptosis [16,17,19,22]. This last hypothesis was supported by the analysis of annexin V expression, showing a dose-dependent increase of the percentage of apoptotic cells in Ukrain-treated ccRCC cells compared with controls.

It was previously shown that UK decreased cell proliferation and increased the blocking of cells in G2/M because of the depolymerization of tubulin [23] and the

Fig. 10

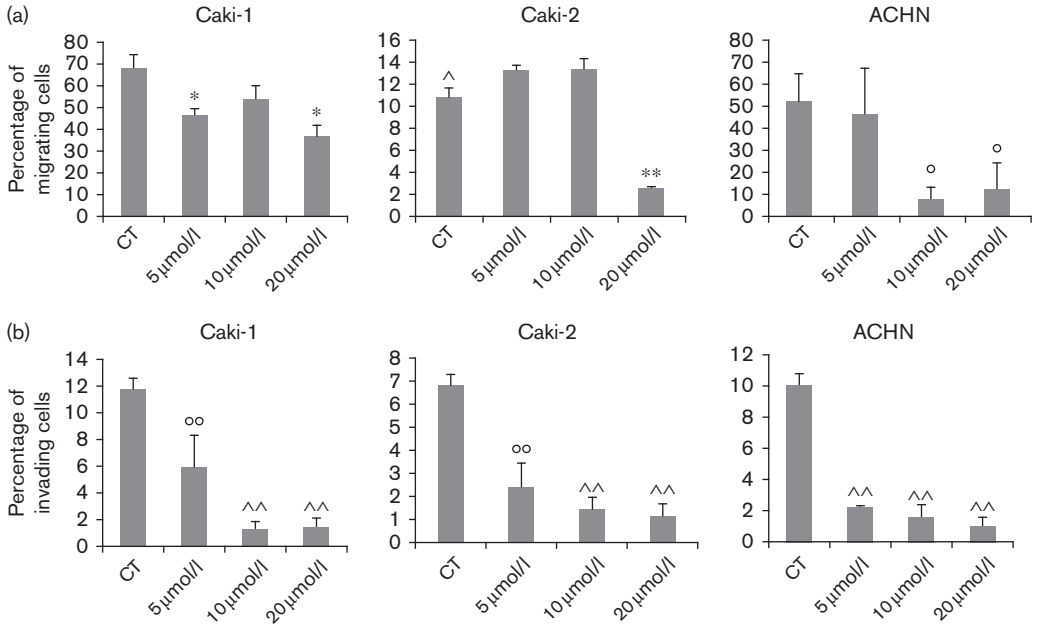

Bar graphs showing the migration (a) and the invasion rate (b) of control (CT) and Ukrain-treated cells. Cells were treated with Ukrain for 48 h. Ukrain significantly reduced the migration rate and the percentage of invading cells in Caki-1, Caki-2, and ACHN. *$P<0.05$ vs. CT; **$P<0.0005$ vs. CT, 5 and 10 μmol/l; ^$P<0.05$ vs. Ukrain 5 and 10 μmol/l; °$P<0.005$ vs. 5 μmol/l; ^^$P<0.005$ vs. CT; and °°$P<0.05$ vs. CT.

consequent 'mitotic slippage'. Our data are discordant as the immunofluorescence analysis showed a well-conserved tubulin cytoskeleton, clearly evident astral microtubules, and the absence of abnormal mitosis, thus suggesting that the antimitotic and the antiproliferative effect of Ukrain is not based on tubulin cytoskeleton alteration.

Cell morphology and epithelial-to-mesenchymal transition

Loss of intercellular adhesion and increased motility promote tumor cell invasion. Acquisition of metastatic phenotype consists of multiple steps, including EMT, which is a complex step-wise process in which the loss of epithelial adhesion, the disruption of basement membrane, and the enhanced migration and invasion are necessary for the completion of the entire mechanism [24]. The loss of cell–cell adhesion is a hallmark of EMT that allows tumor cells to acquire the ability to infiltrate surrounding tissue and metastasize [6]. The graded loss of E-cadherin, the core transmembrane protein of the adherens junctions of differentiated and polarized epithelial cells, correlates with the aggressiveness of numerous carcinomas and the worsening of prognosis, whereas the forced expression of E-cadherin suppresses tumor development in various in-vitro and in-vivo tumor experimental models [25]. Moreover, adherens junctions were dramatically reduced in patients with ccRCC compared with normal tissues [26].

E-cadherin binds catenin that connects the cadherin complex to the actin cytoskeleton. Release of the E-cadherin/β-catenin complex from the membrane has been previously reported to induce cell–cell junction elimination [27] and β-catenin nuclear translocation, in which it may function as a transcriptional coactivator [28].

Our data show that both E-cadherin and β-catenin localization is cytoplasmic in controls ccRCC cells, in contrast with the typical protein localization in the cellular borders and contact sites of differentiated epithelial cells, and that Ukrain is not able to affect their overall expression, or to induce their reexpression at the plasma membrane level, suggesting that Ukrain is not able to modulate these EMT-related phenotype markers at both the considered time points.

We investigated the actin cytoskeleton because changes in the arrangement of actin filaments are common features in cellular transformation [29]. In particular, during EMT dramatic cytoskeleton reorganization occurs, and actin subcortical mesh in epithelial cells is dissociated [30]. We observed diffuse actin stress fibers in controls ccRCC cells. This pattern is not affected by Ukrain in Caki-1 cells. Interestingly, in Caki-2 and ACHN Ukrain administration induced evident actin localization at the cell–cell contacts, suggesting that Ukrain administration may elicit a reorganization of the actin cytoskeleton and the formation of cortical filament bundles, typical of the epithelial phenotype. As in transformed

Fig. 11

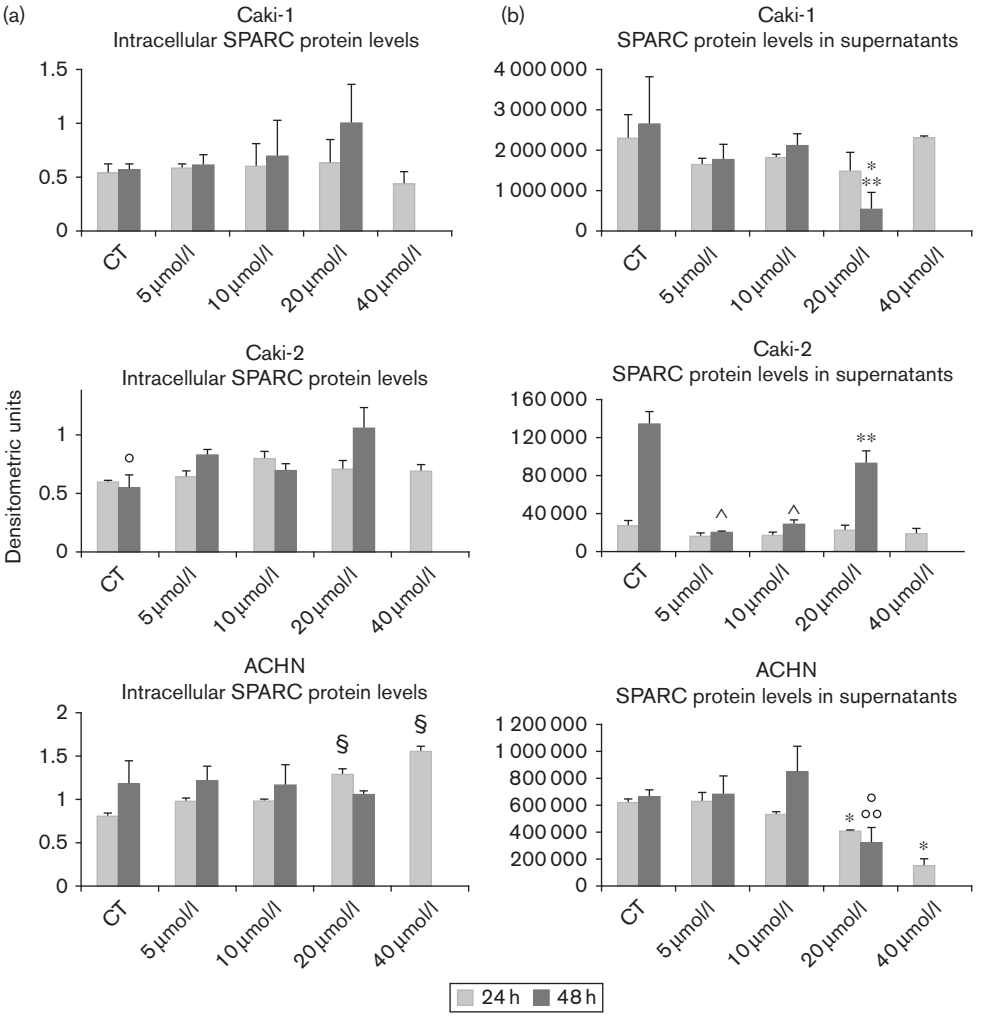

Bar graphs showing secreted protein acidic and rich in cysteine (SPARC) protein levels in cell lysates (a) and secreted in cell supernatants (b). Data were obtained after densitometric scanning of immunoreactive bands and are expressed as densitometric units. This pattern of SPARC protein levels suggests that 48 h after administration Ukrain is able to concomitantly and specifically target extracellular and intracellular SPARC, reducing extracellular matrix remodeling in the tumor environment and possibly reducing cell proliferation. Data were obtained from three independent experiments for samples run in duplicate and are expressed as densitometric units ± standard deviation. $^{\S}P<0.05$ vs. control (CT) and 10 and 5 µmol/l, $^{*}P<0.005$ vs. CT; $^{**}P<0.05$ vs. 10 and 5 µmol/l; $^{\wedge}P<0.0005$ vs. CT; $^{\circ}P<0.05$ vs. CT; and $^{\circ\circ}P<0.005$ vs. 10 and 5 µmol/l.

Table 1 Percentage of control and Ukrain-treated clear cell renal cell carcinoma cells in the G2/M phase of the cell cycle analyzed by flow cytometry

	Caki-1	Caki-2	ACHN
Control	6.6	3.3	12
5 µmol/l	6.9	8.2	14.6
10 µmol/l	15.1	8.7	20.3
20 µmol/l	36	15	49.2

cells a crucial alteration of the actin cytoskeleton results in the disappearance of the marginal actin filament bundles consistent with a decrease of cell–cell adhesion and with an alteration of the motile behavior of epithelial cells [31], our data on Caki-2 and ACHN are indicative of cells that show a polarity, although Ukrain did not modify E-cadherin/β-catenin immunoreactivity.

Vimentin is a widely used marker of EMT. Silencing vimentin causes mesenchymal cells to adopt epithelial shapes, and following transfection with vimentin cDNA epithelial cells adopt mesenchymal shapes coincident with vimentin intermediate filaments assembly. The induction of EMT in Madin–Darby canine kidney cells is characterized by decreased E-cadherin expression, by increased vimentin expression [32], and by increased cell motility [33]. Several studies have shown that vimentin upregulation in carcinomas correlates with parameters of malignancy such as tumor grade and survival incidence [34], and RCC is reported to constantly express vimentin

[35]. Here, we show that Ukrain is not able to decrease vimentin expression in ccRCC cells. However, in some Caki-1 and ACHN cells we observed a denser perinuclear localization of vimentin intermediate filaments starting after 5 μmol/l Ukrain administration. This rearrangement is consistent with the failure to form extended filaments and with vimentin downregulation, and is concomitant with the actin cytoskeleton arrangement in the same cells forming subcortical bundles just beneath the plasma membrane, typical of the epithelial phenotype. These findings suggest for some Ukrain-treated cells a tendency to switch from mesenchymal to epithelial-like phenotype, also in agreement with the results of the morphological analysis.

Considered as a whole, data on the EMT-related phenotype suggest a cell-type-based response. In all the considered cell lines, Ukrain did not modify E-cadherin/β-catenin immunoreactivity. Conversely, Ukrain elicited different effects on cytoskeleton arrangement. Ukrain induced a reorganization of actin cytoskeleton in Caki-2 and not in Caki-1, while the drug had the opposite effect on vimentin expression. In ACHN, both actin and vimentin are affected by Ukrain starting after administration of the lower dose, suggesting that ACHN cells likely respond to a higher extent acquiring an epithelial-like phenotype.

To further discuss these data on EMT markers and cell morphology, we can provide a further consideration, on the basis of the evidence that it was shown that invasive and metastatic epithelial cells show a well-differentiated phenotype characterized by the expression of E-cadherin [36]. This can be explained as an incomplete EMT, thereby suggesting that the transition to an aggressive malignant phenotype is not an 'all or nothing' event, but rather a multistep process that manifests in a broad range of phenotypic changes [37]. Moreover, the steps characterizing the EMT multistep process do not necessarily occur consecutively and are not all necessarily present in a given sample of EMT. On the basis of these suggestions, we can hypothesize that Ukrain may revert the malignant phenotype of ccRCC cells by modification of the actin and vimentin cytoskeleton leading to a more epithelial-like polarized phenotype, although in these cells the pattern of expression of E-cadherin/β-catenin complex is not affected.

Matrix metalloproteinases activity and invasive potential

Disturbances of the finely tuned homeostasis of ECM may have significant roles in many diseases, such as fibrosis, and in tumor progression [38]. The physical processes of tumor invasion, which involves disengagement of the cells from their microenvironment, followed by breakdown of the surrounding ECM, cell movement, and reestablishment of the local environment at a new site, enable cancer cells at the tumor-invasive front to overcome the ECM barrier, and penetrate adjacent tissues. This is accomplished by an ECM remodeling process involving MMPs and SPARC [39].

MMPs are key markers of EMT, and in-vitro studies showed that ECM remodeling and proteolytic degradation of ECM by MMPs are major steps in tumor invasion [40], leading to cancer cell dissemination and metastases. We aimed at analyzing whether Ukrain is able to affect the expression of the gelatinases MMP-2 and MMP-9, playing a relevant role during tumor invasion, because of their activity in degrading type IV collagen of basement membranes [41].

In RCC, upregulation of the MMP-2 and MMP-9 proteins correlates with poor prognostic variables [42]. Patients with ccRCC with high MMP-2 activation ratio or high MMP-9 had a significantly worse outcome [43], and poor survival with high frequency of metastases is associated with MMP-9 activity [44,45]. However, both MMP-2 and MMP-9 seem engaged in the promotion and progression of RCC [42].

In particular, patients with RCC with involvement of major veins or invasion to perinephric tissues had higher expression of active MMP-2 than those whose tumors were limited to the kidneys [43]. This supports the key role of MMPs in tumor invasion and metastasis. Interestingly, a tendency to higher expression and activation of MMP-2 was described in T3 tumors, compared with T1 and T2, leading to the hypothesis that MMP-2 may play a key role in initiating RCC metastasis [43].

The overall pattern of protein expression of MMP-2 and MMP-9 shows that Ukrain is able to significantly decrease their activity 48 h after administration, suggesting that Ukrain could modulate the invasive potential of ccRCC cells. This suggestion was strongly confirmed by the invasion assay on matrigel, showing that Ukrain-treated cells show a less invasive potential.

Secreted protein acidic and rich in cysteine protein expression

Tumor invasion and metastasis occur in the context of the ECM, and the cellular interactions with ECM are mediated by SPARC, a matricellular glycoprotein involved in several biological processes involving ECM remodeling [46,47]. SPARC is highly expressed in a wide range of human malignant tumors, and its deregulated expression is often correlated with disease progression and/or poor prognosis [48–53]. Although SPARC is generally overexpressed in malignant tumors, it was shown that SPARC has a tumor-suppressor function in ovarian cancer cells [54]. Thus, the biological properties of SPARC may be variable among different cancer types.

SPARC shows de-adhesive properties through an antagonistic action involving integrin signaling [55], allowing

the regulation of cell–matrix interactions. In the mechanisms leading to tumor invasion, the ability of the tumor cell to migrate and invade the surrounding environment is dependent on the modulation of the interactions between tumor cells and ECM components. Therefore, SPARC may have a functional role during tumor cell invasion into adjacent tissues.

Our results show that the secreted SPARC protein levels are significantly downregulated by Ukrain in the supernatants of all the considered cell lines, suggesting that Ukrain may be effective to reduce the ECM remodeling, thus rendering the tumor microenvironment less permissive to tumor invasion and migration.

SPARC expression in cell lysates has an opposite pattern of expression compared with the secreted protein. In fact, our results show that SPARC intracellular protein levels, although unchanged in ACHN after Ukrain treatment, were increased in Caki-1 and Caki-2 48 h after Ukrain administration. This is a very interesting finding, as SPARC is also a potent antiproliferative agent because of its ability to inhibit the cell cycle [56]. Intracellular SPARC downregulation, because of the methylation of its promoter, was previously described in human ovarian cancer [57,58], and was related to increased proliferation and cell cycle progression [56]. Therefore, high levels of intracellular SPARC induced by Ukrain administration may be related to a reduced ability of cells to enter the cell cycle, and as a consequence, to a reduced cell proliferation [59].

Our data on intracellular SPARC levels are consistent with the cell cycle analysis showing that a considerable number of Ukrain-treated cells were arrested in the G2/M phase, and provide strong evidence that Ukrain may contribute to induce cell cycle arrest, and in turn the inhibition of cell division in ccRCC cells. However, further studies are needed to weight a possible link between SPARC intracellular levels and reduced cell proliferation after Ukrain administration.

The overall SPARC expression suggests that Ukrain is able to target extracellular and intracellular SPARC, reducing ECM remodeling in the tumor environment and possibly reducing cell proliferation. This hypothesis is based on the suggestion that SPARC may elicit different effects extracellularly and intracellularly, according to the finding that SPARC may be translocated into the nucleus after endocytosis [60], where the protein may exert its effects on cell cycle. However, the complex mechanisms leading to concomitantly different intracellular and secreted SPARC levels remain an open question.

Conclusion

Considered as a whole, our results suggest that Ukrain may exert relevant effects on ccRCC progression. In particular, we show that Ukrain targets some EMT markers in ccRCC cells leading to the acquisition of an epithelial-like phenotype induced by Ukrain administration, and strongly affects two major aspects involved in RCC tumorigenesis, which are ECM remodeling and cell proliferation.

Acknowledgement

Conflicts of interest

The authors declared no competing interests.

References

1 Cohen HT, McGovern FJ. Renal-cell carcinoma. *N Engl J Med* 2005; **353**:2477–2490.
2 Zisman A, Pantuck AJ, Wieder J Chao DH, Dorey F, Said JW, *et al.* Risk group assessment and clinical outcome algorithm to predict the natural history of patients with surgically resected renal cell carcinoma. *J Clin Oncol* 2002; **20**:4559–4566.
3 Thiery JP. Epithelial-mesenchymal transitions in tumour progression. *Nat Rev Cancer* 2002; **2**:442–454.
4 Kang Y, Massagué J. Epithelial–mesenchymal transitions: twist in development and metastasis. *Cell* 2004; **118**:277–279.
5 Hendrix MJC, Luo J, Seftor EA, Sharma N, Heidger PM Jr, Cohen MB, *et al.* Epithelial–mesenchymal molecular interactions in prostatic tumor cell plasticity. In: Ablin RJ, Mason MD, editors. *Metastasis of prostate cancer.* Dordrecht, The Netherlands: Springer Academic Publishers; 2007. pp. 127–141.
6 Lee JM, Dedhar S, Kalluri R, Thompson EW. The epithelial–mesenchymal transition: new insights in signaling, development, and disease. *J Cell Biol* 2006; **172**:973–981.
7 Kretmair H. Hypericum perforatum, St John's wort. *Pharmazie* 1950; **5**:85–88.
8 Susak YM, Zemskov VS, Yaremchuk OY, Kravchenco OB, Yatsyk IM, Korsh OB. Comparison of chemotherapy and X-ray therapy with Ukrain monotherapy for colorectal cancer. *Drugs Exp Clin Res* 1996; **22**:115–122.
9 Uglianitsa KN, Nechiporenko NA, Nefyodov LI, Brzosko WJ. Ukrain therapy of stage T1N0M0 bladder cancer patients. *Drugs Exp Clin Res* 1998; **24**:227–230.
10 Uglianitsa KN, Nefyodov LI, Brzosko W. Evaluation of the efficacy of Ukrain in the treatment of breast cancer: clinical and laboratory studies. *Drugs Exp Clin Res* 1998; **24**:231–239.
11 Zemskov V, Prokopchuk O, Susak Y, Zemskov S, Tkachenko O, Hodysh Y, *et al.* Efficacy of Ukrain in the treatment of pancreatic cancer. *Langenbecks Arch* 2002; **387**:84–89.
12 Ernst E, Schmidt K. Ukrain–a new cancer cure? A systematic review of randomised clinical trials. *BMC Cancer* 2005; **5**:69.
13 Gansauge F, Ramadani M, Schwarz M, Beger HG, Lotspeich E, Poch B. The clinical efficacy of adjuvant systemic chemotherapy with gemcitabine and NSC-631570 in advanced pancreatic cancer. *Hepatogastroenterol* 2007; **54**:917–920.
14 Funel N, Costa F, Pettinari L, Taddeo A, Sala A, Chiriva-Internati M, *et al.* Ukrain Affects Pancreas Cancer Cell Phenotype in vitro by Targeting MMP-9 and Intra-/Extracellular SPARC Expression. *Pancreatology* 2010; **10**:545–552.
15 Liepins A, Nowicky JW. Activation of spleen cell lytic activity by the alkaloid thiophosphoric acid derivative: Ukrain. *Int J Immunopharmac* 1992; **14**:1437–1442.
16 Liepins A, Nowicky JW, Bustamante JO, Lam E. Induction of bimodal programmed cell death in malignant cells by the derivative Ukrain NSC-631570. *Drugs Exp Clin Res* 1996; **22**:73–79.
17 Roublevskaia IN, Polevoda BV, Ludlow JW, Haake AR. Induced G2/M arrest and apoptosis in human epidermoid carcinoma cell lines by semisynthetic drug Ukrain. *Anticancer Res* 2000; **20**:3163–3167.
18 Habermehel D, Kammerer B, Handrick R, Eldh T, Gruber C, Cordes G, *et al.* Proapoptotic activity of Ukrain is based on Chelidonium majus L. alkaloids and mediated via a mitochondrial death pathway. *BMC Cancer* 2006; **6**:14.
19 Gagliano N, Moscheni C, Torri C, Donetti E, Magnani I, Costa F, *et al.* Ukrain modulates glial fibrillary acidic protein, but not connexin 43 expression, and induces apoptosis in human cultured glioblastoma cells. *Anticancer Drugs* 2007; **18**:669–676.
20 Erba E, Bassano L, Di Liberti G, Muradore I, Chiorino G, Ubezio P, *et al.* Cell cycle phase perturbations and apoptosis in tumour cells induced by aplidine. *Br J Cancer* 2002; **86**:1510–1517.

21 Trevor KT, McGuire JG, Leonova E. Association of vimentin intermediate filaments with the centrosome. *J Cell Science* 1995; **108**:343–356.
22 Nowicky JW, Hiesmayr W, Nowicky W, Liepins A. Influence of Ukrain on DNA, RNA and protein synthesis in malignant cells. *Drugs Exp Clin Res* 1996; **22**:81–91.
23 Panzer A, Joubert AM, Bianchi PC, Hamel E, Seegers JC. The effects of chelidonine on tubulin polymerisation, cell cycle progression and selected signal transmission pathways. *Eur J Cell Biol* 2001; **80**:111–118.
24 Yang J, Liu Y. Dissection of key events in tubular epithelial to myofibroblast transition and its implications in renal interstitial fibrosis. *Am J Pathol* 2001; **59**:1465–1475.
25 Nelson WJ, Nusse R. Convergence of Wnt, beta-catenin, and cadherin pathways. *Science* 2004; **303**:1483–1487.
26 Kim G, Rajasekaran SA, Thomas G, Rosen EA, Landaw EM, Shintaku P, *et al.* Renal clear-cell carcinoma: an ultrastructural study on the junctional complexes. *Histol Histopathol* 2005; **20**:35–44.
27 Marambaud P, Shioi J, Serban G, Georgakopoulos A, Sarner S, Nagy V, *et al.* A presenilin-1/gamma-secretase cleavage releases the E-cadherin intracellular domain and regulates disassembly of adherens junctions. *EMBO J* 2002; **21**:1948–1956.
28 Van Es JH, Barker N, Clevers H. You WNT some, you lose some: oncogenes in the WNT signaling pathway. *Curr Opin Genet Dev* 2003; **13**:28–33.
29 Pawlak G, Helfman DM. Cytoskeletal changes in cell transformation and tumorigenesis. *Curr Opin Genet Dev* 2001; **11**:41–47.
30 Savagner P. Leaving the neighborhood: molecular mechanisms involved during epithelial-mesenchymal transition. *Bioessays* 2001; **23**:912–923.
31 Ayollo DV, Zhitnyak IY, Vasiliev JM, Gloushankova NA. Rearrangements of the actin cytoskeleton and E-cadherin-based adherens junctions caused by neoplasic transformation change cell–cell interactions. *PLoS One* 2009; **4**:e8027.
32 Martel C, Harper F, Cereghini S, Noë V, Mareel M, Crémisi C. Inactivation of retinoblastoma family proteins by sv4o t antigen results in creation of a hepatocyte growth factor/scatter factor autocrine loop associated with an epithelial-fibroblastoid conversion and invasiveness. *Cell Growth Differ* 1997; **8**:165–178.
33 Mendez MG, Kojima S-I, Goldman RD. Vimentin induces changes in cell shape, motility, and adhesion during the epithelial to mesenchymal transition. *FASEB J* 2010; **24**:1838–1851.
34 Hendrix MJC, Seftor EA, Chu YW, Trevor KT, Seftor RE. Role of intermediate filaments in migration, invasion and metastasis. *Cancer Metast Rev* 1996; **15**:507–525.
35 Iyer PV, Leong AS. Poorly differentiated squamous cell carcinomas of the skin can express vimentin. *J Cutan Pathol* 1992; **19**:34–39.
36 Rajasekaran SA, Gopal J, Espineda C, Ryazantsev S, Schneeberger EE, Rajasekaran AK. HPAF-II, a cell culture model to study pancreatic epithelial cell structure and function. *Pancreas* 2004; **29**:e77–e83.
37 Christiansen JJ, Rajasekaran AK. Reassessing epithelial to mesenchymal transition as a prerequisite for carcinoma invasion and metastasis. *Cancer Res* 2006; **66**:8319–8326.
38 Kessenbrock K, Plaks V, Werb Z. Matrix metalloproteinases: regulators of the tumor microenvironment. *Cell* 2010; **141**:52–67.
39 McCawley LJ, Matrisian LM. Matrix metalloproteinases: multifunctional contributors to tumor progression. *Mol Med Today* 2000; **6**:149–156.
40 Liotta LA, Stetler-Stevenson WG. Tumor invasion and metastasis: an imbalance of positive and negative regulation. *Cancer Res* 1991; **51**:5054s–5059s.
41 Collier IE, Wilhelm SM, Eisen AZ, Marmer BL, Grant GA, Seltzer JL, *et al.* H-ras oncogene transformed human bronchial epithelial cells (TBE-1) secrete a single metalloproteinase capable of degrading basement membrane collagen. *J Biol Chem* 1988; **263**:6579–6587.
42 Kallakury BV, Karikehalli S, Haholu A, Sheehan CE, Azumi N, Ross JS. Increased expression of matrix metalloproteinases 2 and 9 and tissue inhibitors of metalloproteinases 1 and 2 correlate with poor prognostic variables in renal cell carcinoma. *Clin Cancer Res* 2001; **7**:3113–3119.
43 Takahashi M, Oka N, Naroda T, Nishitani MA, Kanda K, Kanayama HO, *et al.* Prognostic significance of matrix metalloproteinases-2 activation ratio in renal cell carcinoma. *Int J Urol* 2002; **9**:531–538.
44 Kawata N, Nagane Y, Igarashi T, Hirakata H, Ichinose T, Hachiya T, *et al.* Strong significant correlation between MMP-9 and systemic symptoms in patients with localized renal cell carcinoma. *Urology* 2006; **68**: 523–527.
45 Kawata N, Nagane Y, Hirakata H, Ichinose T, Okada Y, Yamaguchi K, *et al.* Significant relationship of matrix metalloproteinase 9 with nuclear grade and prognostic impact of tissue inhibitor of metalloproteinase 2 for incidental clear cell renal cell carcinoma. *Urology* 2007; **69**:1049–1053.
46 Bradshaw AD, Sage EH. SPARC, a matricellular protein that functions in cellular differentiation and tissue response to injury. *J Clin Invest* 2001; **107**:1049–1054.
47 Brekken RA, Sage EH. SPARC, a matricellular protein: at the crossroads of cell-matrix communication. *Matrix Biol* 2000; **19**:569–580.
48 Wewer UM, Albrechtsen R, Fisher LW, Young MF, Termine JD. Osteonectin/SPARC/BM-40 in human decidua and carcinoma, tissues characterized by de novo formation of basement membrane. *Am J Pathol* 1988; **132**:345–355.
49 Porte H, Chastre E, Prevot S, Nordlinger B, Empereur S, Basset P, *et al.* Neoplastic progression of human colorectal cancer is associated with overexpression of the stromelysin-3 and BM-40/SPARC genes. *Int J Cancer* 1995; **64**:70–75.
50 Ledda F, Bravo AI, Adris S, Bover L, Mordoh J, Podhajcer OL. The expression of the secreted protein acidic and rich in cysteine (SPARC) is associated with the neoplastic progression of human melanoma. *J Invest Dermatol* 1997; **108**:210–214.
51 Massi D, Franchi A, Borgognoni L, Reali UM, Santucci M. Osteonectin expression correlates with clinical outcome in thin cutaneous malignant melanomas. *Hum Pathol* 1999; **30**:339–344.
52 Thomas R, True LD, Bassuk JA, Lange PH, Vessella RL. Differential expression of osteonectin/SPARC during human prostate cancer progression. *Clin Cancer Res* 2000; **6**:1140–1149.
53 Yamanaka M, Kanda K, Li NC, Fukumori T, Oka N, Kanayama HO, *et al.* Analysis of the gene expression of SPARC and its prognostic value for bladder cancer. *J Urol* 2001; **166**:2495–2499.
54 Yiu GK, Chan WY, Ng SW, Chan PS, Cheung KK, Berkowitz RS, *et al.* SPARC (secreted protein acidic and rich in cysteine) induces apoptosis in ovarian cancer cells. *Am J Pathol* 2001; **159**:609–622.
55 Motamed K, Sage EH. Regulation of vascular morphogenesis by the matricellular protein SPARC. *Kidney Int* 1997; **51**:1383–1387.
56 Rempel SA, Golembieski WA, Fisher JL, Maile M, Nakeff A. SPARC modulates cell growth, attachment and migration of U87 glioma cells on brain extracellular matrix proteins. *J Neurooncol* 2001; **53**:149–160.
57 Said N, Motamed K. Absence of host-secreted protein acidic and rich in cysteine (SPARC) augments peritoneal ovarian carcinomatosis. *Am J Pathol* 2005; **167**:1739–1752.
58 Socha MJ, Said N, Dai Y, Kwong J, Ramalingam P, Trieu V, *et al.* Aberrant promoter methylation of SPARC in ovarian cancer. *Neoplasia* 2009; **11**: 126–135.
59 Funk SE, Sage EH. Differential effects of SPARC and cationic SPARC peptides on DNA synthesis by endothelial cells and fibroblasts. *J Cell Physiol* 1993; **154**:53–63.
60 Gooden MD, Vernon RB, Bassuk JA, Sage EH. Cell cycle-dependent nuclear location of the matricellular protein SPARC: association with the nuclear matrix. *J Cell Biochem* 1999; **74**:152–167.